

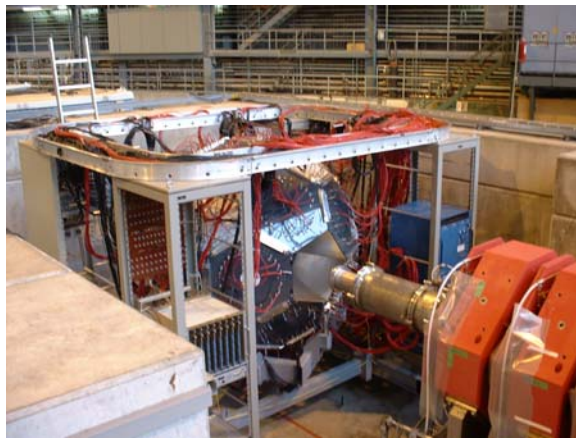
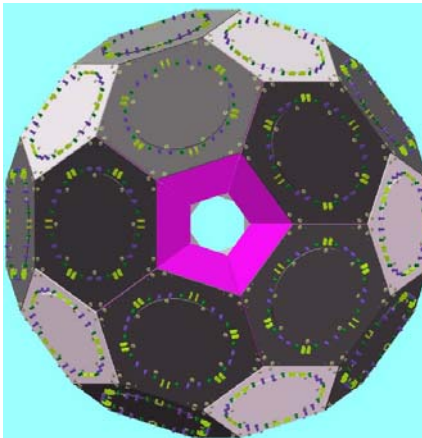
Progress Report 2003 and Beam Request 2004

A Precision Measurement of the Positive Muon Lifetime Using a Pulsed Muon Beam and the μ Lan Detector

PSI Experiment R-99.07; D. Hertzog and R. Carey, co-spokesmen

μ Lan Collaboration 2004: R.M. Carey, S. Cheekatamalla, C. Church, D. Chitwood, M. Clemens, S.M. Clayton, K.M. Crowe, M. D'Antuono, P.T. Debevec, S. Dhamija, W. Earle, A. Gafarov, F.E. Gray, K. Giovanetti, T. Gorringer, S. Hale, M. Hare, D.W. Hertzog, P. Kammel, B. Kiburg, B. Lauss, I. Logachenko, K.R. Lynch, Y. Matus, M. Hance, R. McNabb, J.P. Miller, F. Mulhauser, C.J.G. Onderwater, C.S. Özben, C.C. Polly, S. Rath, B.L. Roberts, D. Webber

(Berkeley, Boston, Illinois, James Madison, Kentucky)



2003: Concept to Reality

Overview

The Muon Lifetime ANalysis (μLan) experimentⁱ aims to measure the positive muon lifetime to 1 ppm precision, thus determining the Fermi coupling constant, G_F , to 0.5 ppm. The experiment requires a high-intensity pulsed muon beam, a symmetric decay spectrometer, a high-precision clock system, and a fast DAQ environment. We have made great strides toward these goals in 2003, which we document in this report. They include:

- Establishment of final $\pi E3$ tune and measurement of extinction factor with real kicker in *dc* mode.
- Construction of kicker beam pipe, electrodes and high-voltage modulators.
- Complete construction of μLan scintillator ball.
- Construction of sulfur targets with a new permanent dipole magnet.
- muSR tests using high-internal-field Arnokrome 3 (AK-3) target.
- Successful use of custom mini-DAQ system based on Midas.
- Installation of experiment and several weeks of production running with *cw* (unkicked) beam. Statistics accumulated equal to current world average.
- Establishment of on-site Project Manager at PSI – Francoise Mulhauser.

Our goals for 2004 are ambitious and anticipate continued success in technical developments. They are to:

- Complete RF shielding of kicker to enable quiet operation.
- Complete the waveform digitizer development and production.
- Complete full Midas-based DAQ with online ROOT analyzer.
- Complete final target / vacuum system components.
- Complete compact high-rate wire chamber for muon beam position monitoring.
- Run to achieve approximately 3 ppm uncertainty on τ_{μ^+} .
- Complete large scale RAID-based distributed data storage system.

We are proud that we have had many undergraduate and graduate students working on this project, including several who will obtain their Ph.D. data from our measurements.

μLan Experimental Concept: A summary included for completeness

The μLan experiment is simple in concept. A stream of approximately 20 muons is brought to rest in a thin target during an accumulation period of several microseconds. The muon beam is then “switched off” and decays are recorded by a surrounding detector during a measuring interval lasting approximately 10 muon lifetimes (22 μs). This cycle is repeated until greater than 10^{12} decays are recorded. The time-structured muon beam must be created artificially at PSI by a installation of a new custom kicker.

During the measuring interval, the Michel positrons are recorded by a multi-segmented, symmetric spectrometer. The geometry features 170 independent scintillator tile pairs, with each element readout by a PMT whose signal is sampled at 500 MHz by a dedicated waveform digitizer. The time of arrival and energy deposited in each tile are derived from a fit to the signal shape. Decay time histograms are constructed from coincident hits and are then fit to extract the lifetime.

The design of the experiment is driven by systematic error considerations. Primary concerns are related to multi-particle pileup, muon spin precession, time-dependence of detector gains or

electronic thresholds, and backgrounds. Pileup is minimized by the segmentation of the detector, the relatively low peak rate per element, and by the double-hit resolution enabled by recording the pulse height in both tile elements for each event. Uncontrolled precession of the stopped, polarized muon ensemble can cause a change in acceptance of the detectors during the measuring interval, which occurs because the emitted positron rate is correlated to the direction of the muon spin. We plan to minimize the residual polarization by using a depolarizing target material, such as sulfur. Further reduction is realized by a systematic dephasing of the initial spins inside a uniform magnetic field. Finally, the detector features front-back matched, symmetric segments, where the sum of elements is nearly immune to a change in spin direction. A new target concept, introduced in 2003, employs Arnokrome 3—a 30% chromium, 10% cobalt, 60% iron composition—having a very high (≈ 1 T) magnetic field. At high field, the muons precess faster than our nominal few nanosecond bin widths.

The instrumentation naturally divides into sub-systems: the muon beam and stopping target, (Illinois); precession magnet and targets (Berkeley), the detector including scintillator tiles, lightguides, PMTs, and mechanical support (Illinois); the calibration system (JMU), the waveform digitizers and clock systems (Boston); and the data acquisition, logging and online analysis computers (Kentucky). Institutions with primary responsibilities for these items are indicated, but much of the work is shared by all collaborators.

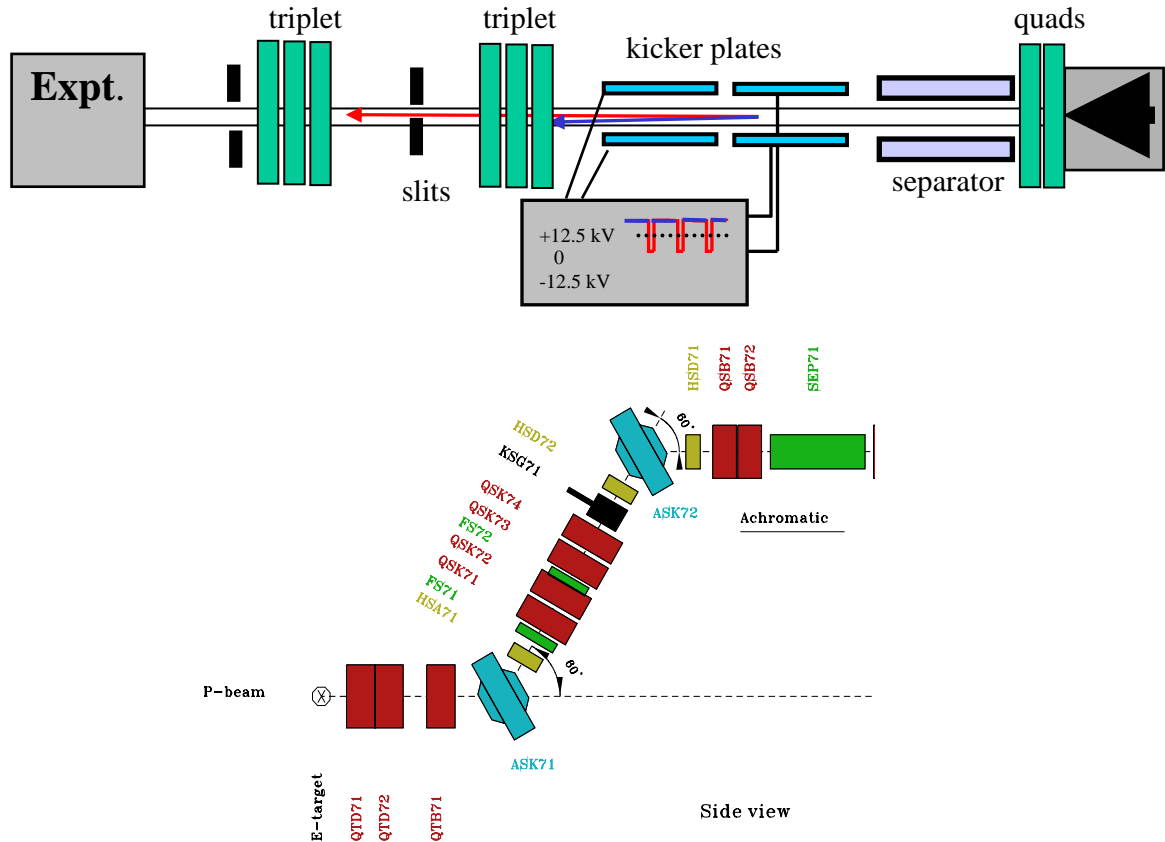


Figure 1. Sketch of beamline components for appendage of $\pi E3$. Beam goes from right to left, with the first quad pair representing QSB71/72 in the standard $\pi E3$ drawings. The $\pi E3$ area has been extended to accommodate the experiment. Lower sketch is the standard $\pi E3$ beamline elements..

The π E3 Beam

Summer 2003 beam line work

For the summer 2003 run the μ Lan Collaboration assembled and tested the extension to the standard π E3 beamline which we need for the precision lifetime measurement. The standard π E3 beam line views the E target at 90° and brings pions and muons produced in the target from target level up to the π E3 area with two anti-symmetric vertical bends. The standard beam line has a physical length of 12.1 m. Our extension adds 11.7 m to the beamline, and the π E3 area was modified substantially in the winter 2003 shutdown to accommodate the added length of the beam line extension and the μ Lan detector. A schematic diagram of our beam line is shown in Figure 1. Several experimental efforts use the π E3 beamline, and the area can usually be reconfigured by the support staff in two days. Assuming that the appropriate electrostatic separator is in the area, our configuration requires two quadrupole triplets, two slit systems, the μ Lan kicker, and the μ Lan detector. Appropriate utilities are available in the area. The beamline assembly is coordinated by PSI staff.

For the lifetime experiment, the *cw* muon beam is chopped—5 μ s on, 22 μ s off—where beam flux is 12 MHz during the on cycle and is reduced by a factor of 1000 during the off cycle. A small and well-contained beam spot is a necessity. The summer 2003 run was the first test with the μ Lan kicker. The important kicker specifications of plate length and electric field had been established in our run in summer 2002. The summer 2002 run also established an appropriate tune for the beam line. The calculated beam envelope of this tune is shown in the figure below.¹ The most important feature of this tune is the small vertical divergence in the region of the separator and the kicker. This small vertical divergence is required for high extinction.

As discussed elsewhere in this report, the kicker could not be operated in a pulsed mode. The kicker was operated in a *dc* mode for extinction measurements. The measured deflection of the beam centroid at the kicker slit as a function of kicker voltage is shown in Figure 2. The width of the kicked beam was typically 2.0 cm. An extinction of a factor of 300 (integral) was obtained with adequate flux and reasonable spot size. Further work is needed to optimize the extinction factor and beam spot. Unfortunately, one of the high-voltage power supplies in the kicker failed while these measurements were in progress. We will complete this program in 2004.

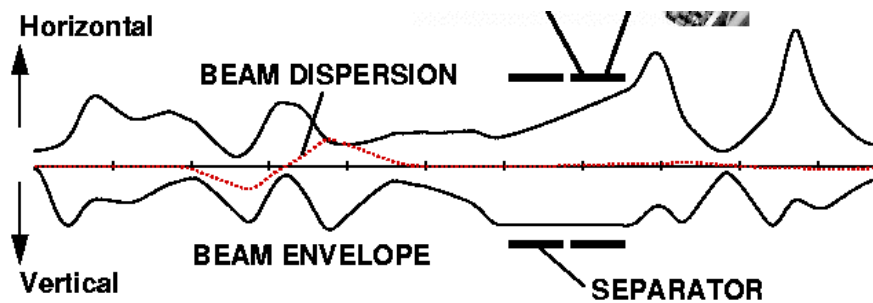


Figure 2 Calculated beam envelope of μ Lan tune for π E3. The beam starts at the target position on the left.

¹ This calculation done with the PSI Graphic Transport code of Dr. Urs Rohrer, which is based on the CERN-SLAC-FERMILAB code of K.L. Brown, D.C. Carey, Ch. Iselin and F. Rothacker. See yellow reports CERN 73-16 (1973) and CERN 80-04 (1980) and http://people.web.psi.ch/rohrer_u/trans.htm.

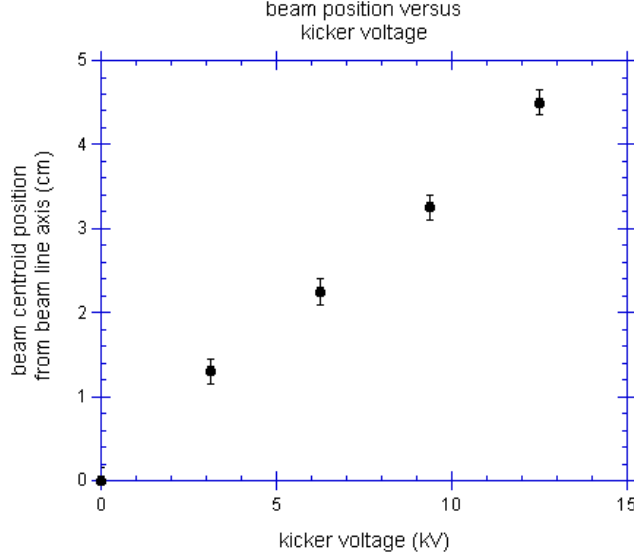


Figure 3. Beam centroid position versus kicker high voltage

Since there are no internal diagnostic elements in the $\pi E3$ beam line, we have devised a systematic turn on procedure by which we verify correct operation of the standard beam line. The first step in the turn on procedure is to establish the ratio of the currents in the bending magnets with no focusing elements on.² The second step is to establish the absolute current settings of the bending magnets by a scan over the surface muon edge with narrow slit settings and no focusing elements on.³ The third step is to turn on focusing elements and to verify that the beam spot size and rate reproduces previous measurements.⁴ The fourth step is to turn on the separator and to verify that the scan of separator magnetic field for fixed electric field reproduces previous measurements. Since the dispersion in the beam line is in the vertical, we use a vertical separator and we kick the beam in the vertical plane.

We measure beam profiles and rates in air downstream of a vacuum window. We made measurements at two positions in this run: at the focus of the first quadrupole triplet and at the focus of the second quadrupole triplet. The kicked beam is lost on slits which are at the first focus. The beam spot and rate on target is largely determined by the beam at the kicker slits. The stopping target for the μLan experiment is at the second focus.

A semi-quantitative beam profile is obtained with a wire chamber beam profile monitor. This device provides a good measurement of the beam centroid and the beam width, but the signal to noise is too poor to measure the beam profile far from the peak. For the summer, 2003 run a more accurate beam profile was obtained by scanning the beam with small area thin scintillators. The two dimensional translation stage was made by PSI. This method provides muon-electron discrimination and can measure beam halo. A typical beam profile is shown in the figure below.

² We have found empirically that this ratio depends significantly on the settings of the slits between the two bends.

³ With no focusing elements on, the momentum acceptance of the beam line is of the order of 1%. With focusing elements on, the momentum acceptance depends on the tune and is of the order 4%.

⁴ With all focusing elements on, a scan over the surface muon peak finds that the maximum flux occurs at a current in the dipoles, which depends on the slit settings and is lower than the peak momentum expectation by as much as 8%.

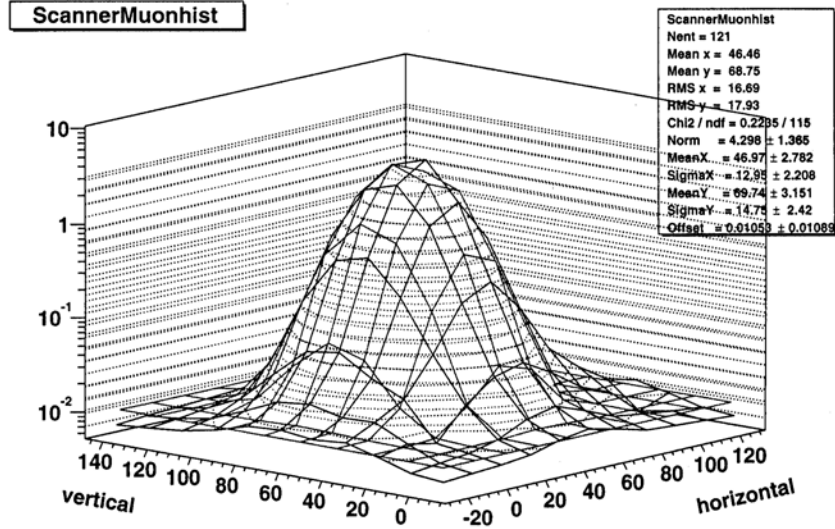


Figure 4. Beam profile at vacuum window exit obtained with scintillator scan.

The muon flux is often too large to be counted directly. We use a scintillator telescope to count the Michel electrons and calibrate the telescope against an in-beam detector. In this run we used three telescopes with different solid angles, which viewed the stopping target from different angles, to verify our flux measurements. With all beam line slits open we had a flux of 45 MHz at the kicker slit. We use the beam line slits to reduce this flux to the 12 MHz that we need for μLan . At this flux we have a beam spot with horizontal and vertical widths (sigma) of 1.28 cm and 1.18 cm, respectively, at the position of the kicker slit. The measured beam rate vs. slit setting is shown in Figure 5.

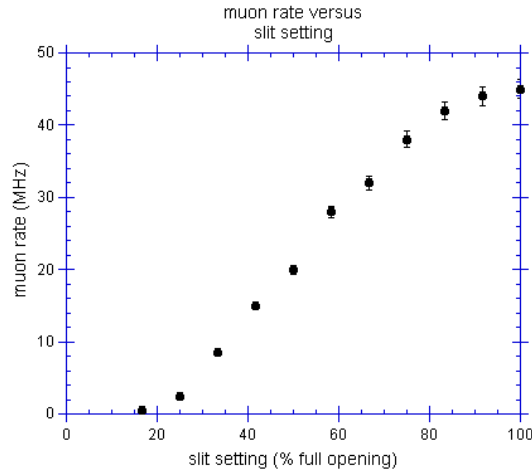


Figure 5. Muon rate vs. slit setting.

The standard PSI vacuum window is 190 μm for the 30 cm diameter beam pipe and 126 μm for the 16 cm diameter beam pipe. The multiple scattering of low-energy muons in these windows is significant, about 40 mrad. In addition to the vacuum window we expect to use some

type of in-beam detector, a scintillator or a wire chamber, which increases the material through which the muons must pass. Since the distance from the vacuum window to the center of the μ Lan detector and the stopping target is 40 cm, the beam spot size increases. In addition to the multiple scattering, the material degrades the energy of the muons. Particles could range out before the stopping target, or miss the stopping target and range out in the air, or stop in the detector. All of these muons will produce asymmetries in the detector counting rates. We have addressed these concerns by measuring the multiple scattering in mylar and iron foils of appropriate thicknesses. These measurements were compared to calculations done with the SRIM code.⁵ Agreement with the SRIM calculation is fair as shown in Figure 6.

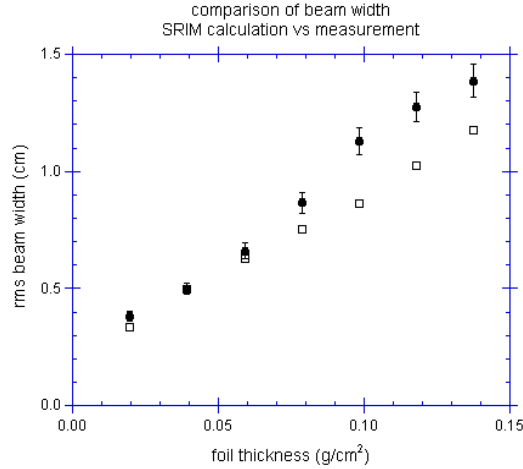


Figure 6. Comparison of measured and calculated spot size versus foil thickness.

A vexing concern is the possibility of a low-momentum component to the muon beam. Since the range of a particle is a strong function of its momentum, $R \propto p^{7/2}$, a low-momentum component may range out before the stopping target. Unfortunately, the standard π E3 beam line is not well configured for momentum analysis.⁶ Absent a high resolution spectrometer, we have devised a simple method to assess the presence of a low-momentum tail, at least for a negative muon beam. When a negative muon captures in a high-Z material, it does not produce a Michel electron. Thus when we place a thin iron foil in front of a plastic stopping target, we only count Michel electrons from muons that stop in the plastic. Muons stopping in the iron give no signal. As the thickness of the iron foil increases, the low-momentum tail no longer stops in the plastic. This method was tested with a stack of 25 μ m-thick foils. We need thinner foils for a quantitative measurement.

New Kicker

The μ Lan kicker represents one of the greatest challenges to our effort. It sits just downstream of the electrostatic separator and consists of 0.75 m long by 20 cm wide electrode plates mounted 15 cm apart. Two sets of these plates are operated in series. Opposing plates in a pair are alternatively biased at ± 12.5 kV to deflect the beam into collimators, or to ground to

⁵ SRIM: Stopping and Range of Ions in Matter, by J. F. Ziegler available at <http://www.srim.org>. See also J. F. Ziegler, J. P. Biersack, U. Littmark, The Stopping and Range of Ions in Solids, Pergamon Press, New York (1984).

⁶ The π E3 beam line was designed for pion scattering measurements in conjunction with a magnetic spectrometer in dispersion matched mode. See, for example, Joram et al. Phys Rev C51(1995)2144.

allow the beam to pass undisturbed. The switching network must operate at high frequency in user-triggered patterns and in a “muon-on-demand” mode. The electrodes and the special section of vacuum pipe were fabricated by PSI and were ready for use in July 2003. A photo is shown in Figure 7.

The modulators were designed by Gary Wait and Michael Barnes of TRIUMF and TRIUMF has generously supported their design and development efforts on our behalf. Conceptually, the kicker plates operate rather like a very large oscilloscope deflection circuit. Each charging unit consists of two “stacks” of high voltage MOSFETs connected in a source to drain configuration. The stacks serve as switches, which help conduct charge on and off the kicker electrodes at high frequency. At one moment in an electrode's cycle, the gate voltages of the top stack are high, the MOSFETs are all conducting and the kicker electrode rises to high voltage as current flows through the MOSFET switch. At the same time, the gate voltages of the bottom stack are low, those MOSFETs do not conduct (switch closed) and there is a drop of about 700 V from source to drain on each MOSFET. A moment later in the cycle, the gate voltages are reversed, the top stack becomes an open switch and the bottom stack, now in a conducting state, shorts the charged electrode to ground. At the same time, a similar cycle on the negative electrode brings it back and forth between ground and -12.5 kV, for an overall swing of 25 kV.

Great care must be taken to ensure that the signals arrive at each MOSFET gate within a few ns of each other. Much larger variation in arrival time can lead to large energy losses and could destroy the circuit. The design must keep stray capacitance to a minimum while still keeping RF radiation to acceptable levels. The typical rise and fall times of the electrode voltages are 35-40 ns. These sharp transitions, plus the high voltages involved can create a noise problem for our experiment and those in nearby areas, particularly detection systems working with very small signals.

Working on a very tight time schedule, the TRIUMF team shipped the four cabinets that hold the modulators to PSI in early June for a very encouraging July beam test. With comparatively little effort, we achieved an integrated extinction factor of 300 while retaining a muon rate of 12 MHz. These tests were made by slowly ramping the kicker electrode plates; that is, running in *dc* mode. Still, challenges remain. One of the filter units for a high voltage power supply failed unexpectedly. Filter capacitors should handle the large voltage spikes observed on the line, which were probably responsible for the filter's demise. Furthermore, RF noise generated by the pulsed kicker and carried through the air and over power and ground lines, was unacceptably large.

Since the summer, a small team of μ Lan collaborators, working with Wait and Barnes, have made considerable progress in reducing the noise. To begin with, one of the connecting cables between the two cabinets on each side had been tied to a dirty ground, which made the cable into a very noisy antenna. Moving that connection to a quiet ground reduced the noise voltage on the

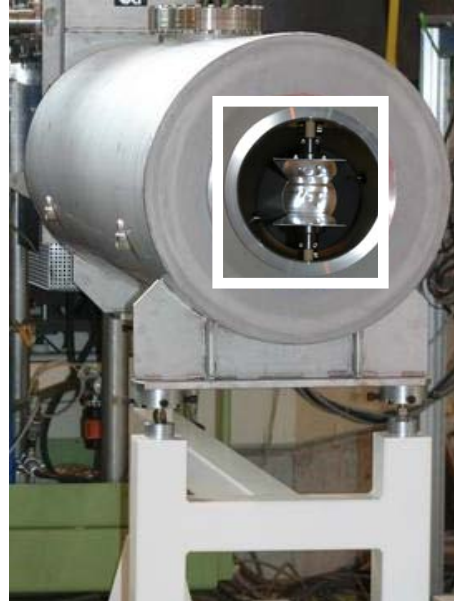


Figure 7. Kicker pipe. Inset, overlaid photo shows kicker plates (orientation is slightly different).

cable by more than an order of magnitude. Improving the electrical contact between the cabinet doors and frame provided only marginal improvement. However, the installation of a Faraday cage surrounding the high voltage MOSFETS in one of the four cabinets plus the further installation of an RF-connector between the cabinet and beam pipe were more promising. In a series of before and after tests on that one cabinet:

- 1) The noise voltage between the cabinet and beampipe was reduced by more than two orders of magnitude.
- 2) The noise voltage on the HV cable braid connecting the cabinets on one side was reduced from 400 volts to 1.3 volts.
- 3) The noise voltage in the main 3-phase power cable was reduced from 7 volts to 1.7 volts.
- 4) The noise voltage going back into the HV power supply in the cabinet was reduced from 350 volts to 67 volts.
- 5) The rise and fall times of the plates were unaffected by the changes.

We will translate these noise reductions into meaningful tests of the remaining noise level by setting up μLan -like detectors in the vicinity of the kicker. We know, for example, that the noise voltage in an antenna mounted a meter from the cabinets saw its noise voltage reduced by a factor of about 6. The kicker beam pipe and modulators are presently being shipped to TRIUMF, where Wait and Barnes plan to make further tests and modifications to the whole assembly. We will be involved to test the noise level with our detectors once improvements are made. The present plan is to complete the changes and ship the kicker system back to PSI in mid summer.

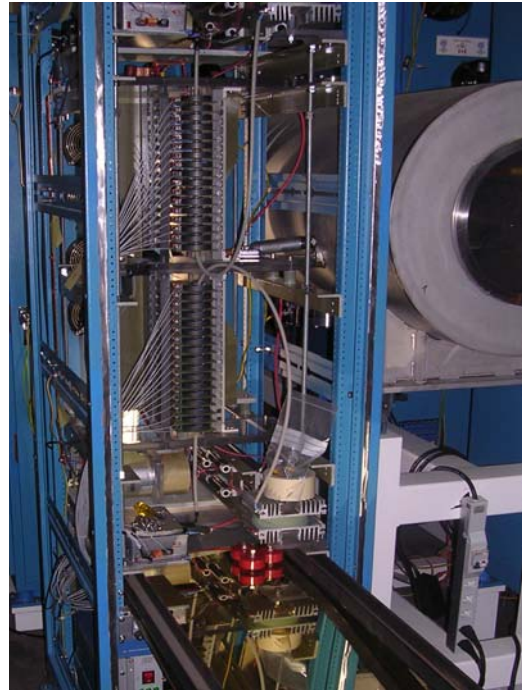


Figure 8. Kicker cabinet opened for installation of internal Faraday cage. MOSFET stacks are visible. End of beampipe is seen on the right.

Detector Construction and Testing

In the summer of 2002, the μLan experiment performed beam studies with 13 percent of the detector completed (44/340 elements). To accomplish our goal of commissioning the full detector for a physics run in the fall of 2003, we needed to fabricate over 300 additional detector elements, ensure the quality of each, design a support structure for the μLan ball, and assemble the entire structure.

The μLan detector is a highly segmented detector consisting of 170 scintillating tile pairs that are nested to ensure coincidences. These elements are arranged to form a truncated icosahedron. This geometric form consists of 20 hexagons and 12 pentagons. To allow entry and exit of the beam, two pentagons are omitted. Each pentagon consists of five triangular tile pair elements and each hexagonal face consists of six triangular tile pair elements.

In order to ensure uniformity in the detectors, a series of tests was performed during the fabrication. Each scintillating tile was glued to a lightguide with an acrylic light mixer at the end,

and the edges of the scintillator were mirrored using an aluminized mylar tape. This was found to increase the light output detected by a photomultiplier tube for a fixed source. We used an ultraviolet light pen to excite the scintillator and measured the light output with one reference tube. By attaching the light source to a motorized stepper, we were able to excite different regions of the scintillator and produce a uniformity distribution. A jig was built to allow for a quick alignment so that the uniformity scans could be compared to identify detectors with similar performance. The bare scintillators have an intrinsic asymmetry, which we reduced by optimizing the wrapping and mirroring procedure. Ultimately, most detectors were uniform to better than 15 percent, and the distributions were recorded with two-dimensional histograms. The number of photoelectrons produced by each detector was then tested in a similar setup that contained a Ru^{106} beta source, collimated and positioned near the center of the detector face. We used a calibrated photoelectron tube to determine the number of photoelectrons produced per detector, establishing the mean number to be approximately 80 pe/mip (Figure 9).

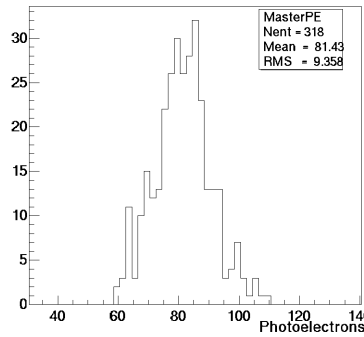


Figure 9. Photoelectron yield for 318 tested scintillator tiles.

After the uniformity scan and photoelectron yield measurement, a photomultiplier tube was glued to the light mixer at the end of the lightguide. A bundle of optical fibers was also attached to the mixer, directed at the tube. The fibers will be used to deliver light to the tube from a calibration LED. Next, each detector element was wrapped in a thin layer of aluminum foil to help improve the light output of the detector, and finally each detector element was wrapped in a layer of tedlar to prevent ambient light from exciting the scintillator.



Figure 10. Detector production and testing in progress.

Detector elements were paired by light uniformity to preserve symmetry in the entire detector. Once all of the pairings had been determined, each element had to be carefully fixed to

a support structure that would hold two nested elements relative to each other. This support structure also provided a standardized way to fix the detector elements in the housing.

The detector houses were constructed upon a steel frame one at a time until the entire “soccer ball” geometry was achieved. Bartoszek Engineering provided the mechanical design for the μ Lan detector assembly and support structure. The support structure is a set of steel rails with a steel frame that has 25 contact points. These contacts can be adjusted to properly align the height and pitch of the detector. Set screws also allow for transverse translation of the detector assembly and rotation about the vertical. The support structure was carefully designed to include 4 racks for the mounting of hardware. During the 2003 run, all of the hardware needed to operate the detectors and read their data was contained within the support structure. This allowed great portability and the convenience of being able to assemble the detector outside of the controlled area, and thanks to the help of the PSI lifting structure, drop it into the beamline almost as easily as the other beamline elements.

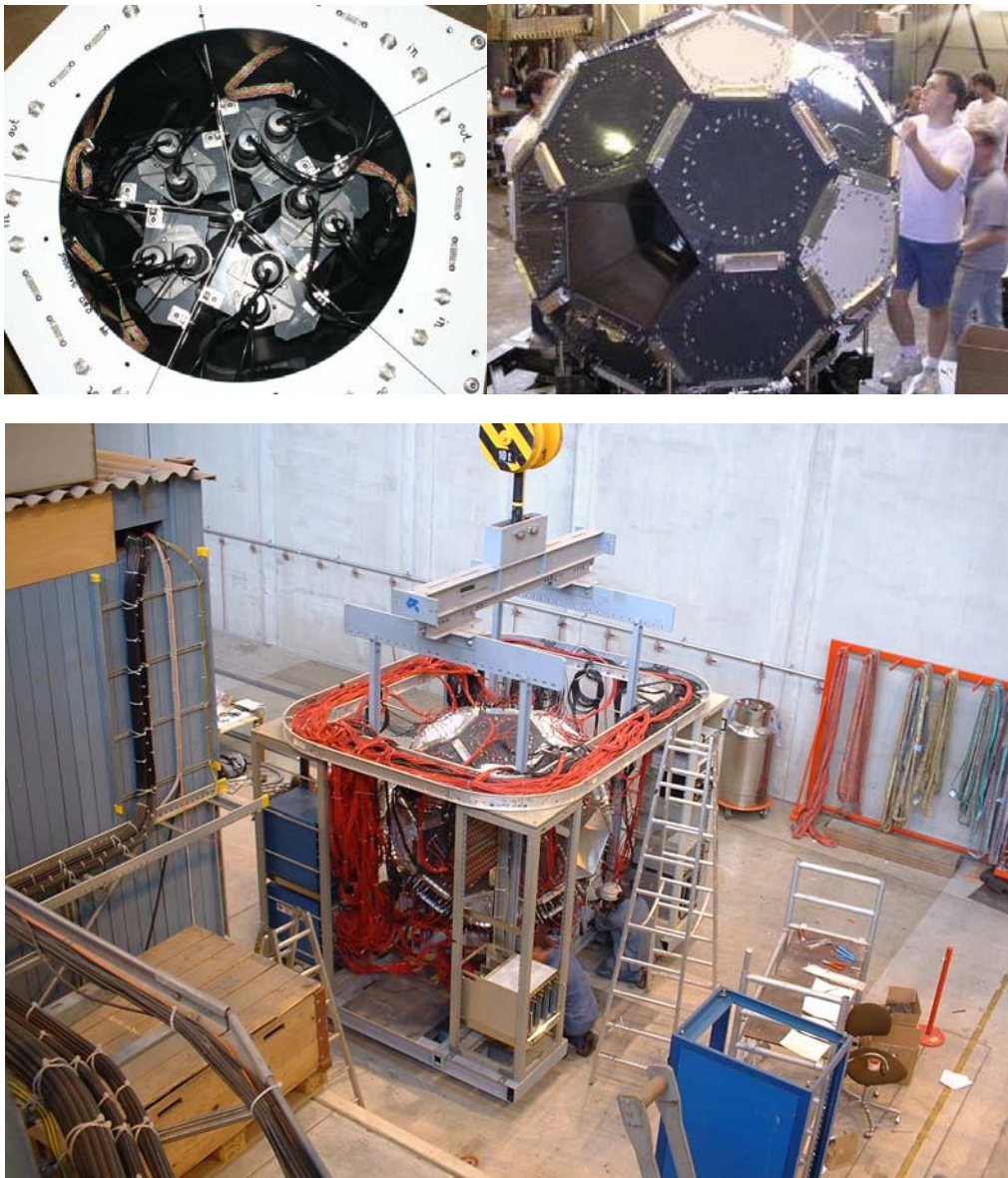


Figure 11. Stages of construction of the μ Lan Ball.

Status of the Custom Electronics

Waveform Digitizers

In previous muon lifetime measurements, and in our Fall 2003 commissioning run, the time of each muon decay was determined by using a TDC to pick off the discriminated signal of the decay positron. At our proposed accuracy of 1 ppm and at the rates we have already achieved for operation in the pulsed mode, the expected "pileup" (where two signals appear as one) systematic error of several ppm is a critical problem. We learned in our related muon g-2 experiment that by sampling the waveform every 2.5 ns, pulses can be separated with confidence when their peak-to-peak separation is as little as 3 ns. For μLan , we are building 500 MHz waveform digitizers and anticipate doing even better. Conceptually, the design of the board is very similar to that of the 400 MHz boards used by g-2. First the signal is sampled by an 8 bit, 500 MHz flash ADC (FADC). The output of FADC is sent to a field programmable gate array (FPGA), where the data is reformatted, given a time stamp, and exported to an external first in-first out (FIFO) memory. The modules sit in a VME-64x crate (slightly modified to provide a few non-standard voltages). Data from each of the modules in a given crate is readout with a Struck PCI-VME interface card at rates up to 80 MBytes/sec. Unlike the g-2 WFD, the dual port FIFOs allow the new board to be readout while data taking continues.

Not only does the new WFD have more onboard memory, faster sampling, and higher readout speed, it is also far more flexible than the old g-2 WFD. By reprogramming the FPGA we can reformat the output data as desired. Indeed, we have defined a number of "personalities" for the board, each of which can be programmed through a JTAG interface, to match the needs of a particular experiment or special data run. Indeed, we plan to use the digitizers in the μCap experiment at PSI as well.

In the summer of 2002, we built a one-channel prototype waveform digitizer board, which successfully sampled and wrote 8-bit samples to memory at 500 MHz. In 2003, we have built a four-channel board like those planned for the experiment, but have struggled to confirm the functionality of the hardware. We have had particular trouble with the VME interface, a relatively simple part of the module, which sits by itself on a small FPGA. In developing code for the FPGA, our engineer had used a standard XILINX tool to simulate the response, including detailed timing, of each part of the circuit. However, despite the fact that the simulation always verified the expected performance of the circuits, tests in the lab often did not concur.

We spent considerable time reviewing the original schematic, the design, layout, and fabrication of the board, the loading of the program into the FPGA (using two different techniques, with identical results). In all cases, everything looked fine. However, in early January 2004, we discovered that the Xilinx simulator we were using to model the behavior of the programmed chip was faulty. With a different simulator (previous versions of which could not be used because they could not handle differential signals) we can now reliably diagnose the detailed timing problems in the logic. In particular, VHDL "case" statements, similar to C "switch-case" constructs, were being incorrectly synthesized, producing no results at all. With a working simulation, we now expect to make rapid progress. It is true that we will have to lay out the four-channel board a second time, but the modifications will be relatively small. By the end of February, we should be able to finish our tests of the four-channel board. If they are successful, we should be able to produce and test the 85 boards needed by the fall.

Clocks and Distribution

To keep systematic errors at 1 ppm or less, the clock error should be 0.1 ppm or smaller. Finding a time base with 0.1 ppm accuracy and stability over months is not a great challenge - vendors such as Precision Test Systems (chosen for g-2) and Agilent (chosen for μLan) can

provide synthesizers driven by ovenized oscillators, which easily meet that specification. In our first experimental run this past fall, we drove the clock distribution system with an Agilent E4400 synthesizer and monitored its output signal by mixing it with another roughly 200 MHz signal from a PTS 3100. The difference frequency was stable at 0.5 Hz over the run. We also measured the outputs of the Agilent and PTS clock signals with a recently calibrated and highly stable frequency counter. The Agilent signal was accurate to 1 part in 100 million while the PTS signal was 1 part in 10 million too high. No frequency drift was observed.

In the future, we may drive the synthesizer with an external time standard, like GPS. However we choose to produce our experimental clock, we have already built a clock distribution system to fan-out clock signals to the 85-odd WFD modules in the final configuration, a system based on that used in g-2 and other precision experiments. The 500 MHz system clock is fanned out by a 1-to-8 splitter/amplifier box and then by six 1-to-16 splitter/amplifier boxes. Another module performs clock division duties by means of ECLinps logic circuits, producing clock signals to drive, for instance, the flight simulator and multi-hit TDC hardware.

To keep the analysis of the lifetime unbiased, we have decided to “hide” the frequency from those determining the lifetime. Instead, they will determine the average lifetime during intervals over which the clock frequency is constant and express their answer in clock units of unknown (to them) magnitude. We employed a version of this “blind operation” in the fall 2003 data taking.

Two other important modules in timing and experimental control are the “flight simulator” and “magic box”. These are both programmable pulse generators with specialized output ports. Our calibration system consists of LEDs mounted next to every detector PMT and a pulsing circuit to drive them. The time pattern of pulses illuminating each PMT will be set by the flight simulator. Like the magic box, which was used to control the operation of the kicker in beam tests this summer, the flight simulator module will be designed around an FPGA which translates commands downloaded from a control PC. In this case, the commands specify the times of hits for each detector channel, either a test pattern for checking continuity or muon decay itself, a more sophisticated test of the data throughput and analysis chain. The translation of commands into hit patterns will be developed on a board very similar to that used for the WFD, but run in reverse. Commands would be downloaded over VME, translated into hit patterns on the FPGA and the patterns themselves would come out through a front panel ribbon cable, which would replace the input connectors and flash ADCs on the WFD board.

Status of Data Acquisition System and Offline Processing

During 2003 our DAQ efforts were largely focused on two tasks. First was continuing development work on the data acquisition for the full μ Lan setup, which involves a high-rate pulsed muon beam and pulse-shape decay electron readout. Second was parallel development work on a data acquisition for the 2003 engineering running, which used a low-rate continuous muon beam and multi-hit TDC decay-electron readout.

For the pulsed-beam configuration, we have constructed an acquisition comprised of a local network of eight frontend processors, one backend processor, and several disk arrays for data storage. The frontend processors each provide the readout for one VME crate containing the CAEN multi-hit TDCs that instrument the muon beam detectors, six VME crates containing the BU waveform digitizers that instrument the decay electron detectors, and various interfaces for controlling and monitoring the beam-line elements, high voltage supplies, etc. The waveform digitizer frontends are designed to process the raw pulse-shape data into compressed pulse-parameter data, thus reducing the raw data rate of about 50 MB/sec on the VME side to a compressed data rate of about 5 MB/sec on the backend side. The backend processor is responsible for assembling the individual data fragments from the eight front processors and the data transfer to the disk arrays. The acquisition is designed to accumulate the experimental data in

deadtimeless segments of lengths 10-100 ms. It was developed from the MIDAS software package with a distributed, modular design philosophy.

During 2003 we assembled the DAQ hardware and developed a basic driver routine for the multi-hit TDCs, a basic compression routine for the waveform digitizers, and a method for multi-processor event synchronization. We conducted a series of rate measurements with fake data to test our design. Future tasks include: upgrading the multi-hit TDC drivers, developing the waveform digitizer drivers, and developing the synchronization between the data acquisition with the pulsed beam.

In addition, in 2003 we developed and operated a multi-hit TDC-based acquisition for our 2003 low-rate continuous beam run. The acquisition also employed a distributed, modular approach with three frontend processors, one for the multi-hit TDC readout, one for the waveform digitizer readout, and one for control and monitoring. A backend processor was responsible for assembling the event fragments from each frontend and transferring the data to disk arrays. This 'mini-DAQ' was successful in handling the data rates and synchronizing the frontend processes. However, we did suffer difficulty with the data readout from the multi-hit TDCs. An updated multi-hit TDC driver with hardware error checking status and data integrity analysis will be necessary for the future.

Simulation Effort

In the μ Lan Experiment, two distinct and complementary efforts are being made to model the physics effects using simulations software. The first effort can be called "event-based," and is based on the GEANT4 toolkit. Using a one-at-a-time method of tracking individual particles from the beam line into the detector and simulating their passage through matter volumes, we are able to see the effects of multiple scattering and geometrical obstructions (see Figure 12.) The full complement of relevant physics processes is taken into account by the physics kernel of Geant4. Through this effort we are examining the potential systematic errors caused by scattering and energy loss of the muons and positrons, and by any geometrical asymmetry of the target configurations.

The complementary simulation work uses an "ensemble-based" approach, which is quite different. Here, we focus on synthesizing data sets containing the physics effects of our measurement that are large enough to support fitting procedures and analysis. For example, we will use this method to model the effects of a non-uniform precession field in the target region. The number of individual events needed to make statistical predictions of fit parameters is much larger than can be created using an event-based approach. Therefore, we are developing independent code capable of delivering the same order-of-magnitude statistics as we anticipate achieving in the experimental data set, namely 10^{12} or more.

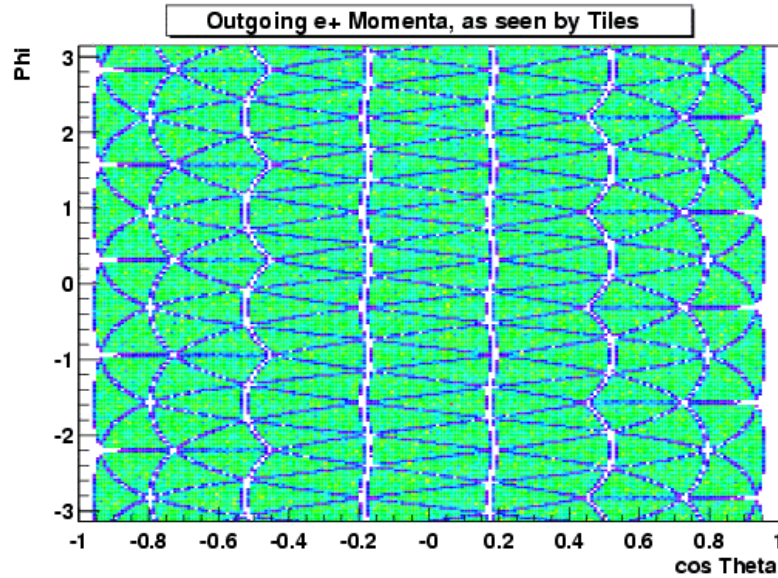


Figure. 12. An acceptance distribution from GEANT for a “bare” target region. Individual triangles represent the tiles in the detector.

Analysis of FALL 2003 Muon Lifetime Data

During the fall run we had the opportunity to accumulate a substantial set of muon lifetime data using the full μLan detector. With the $\pi E3$ *cw* muon source, we collected data with three separate stopping targets under a wide range of incident muon rates. We anticipate that the analysis of this data will lead to an independent measurement of the muon lifetime with an uncertainty of better than 25 ppm. This is to be compared with the previous most accurate measurement and the current world average, which have uncertainties of 27 ppm and 18 ppm, respectively.

Calibration of each of the 340 detector elements was first performed *in situ* using an ADC to measure the light output of each channel and Michel positrons as the source. The procedure was to trigger on the inner detector elements while observing the outer. We varied the HV on the outer element to obtain a gain curve. By observing several elements using an oscilloscope we were able to construct a conversion between ADC value and signal height. This allowed us to set each element to a particular value for an average minimum ionizing particle. The signals were then reversed and the inner detector elements were calibrated. For the majority of our run we used 300 mV/MIP for our detector signals. Figure 13 shows a typical gain curve.

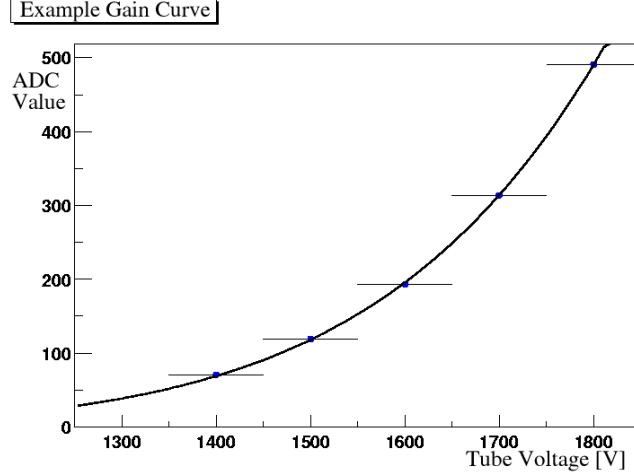


Figure 13. Gain of an individual element vs. high voltage. Data obtained using Michel positrons.

Each channel was individually discriminated with a 50 mV threshold and set with the minimum allowed dead time of 40 ns. The discriminated signals were sent into a CAEN V767 multi-hit TDC to record the time of each decay. Using the Agilent synthesizer running at 200 MHz, we were able to produce a time resolution of about 0.78 ns for each channel.

In addition to the μ Lan detector, we also recorded the time of incoming muons with a CAEN V767 TDC. The signal for the incoming muons was produced from a 500 micron thick sheet of scintillator (T0) sitting just before the target. Using a digital oscilloscope we were able to observe the separation between the beam electrons and muons (see Figure 14). The photomultiplier tubes for measuring the light of the T0 were set such that the beam electrons produced an average pulse of 50 mV and the muons 182 mV. As a systematic check we discriminated the T0 signal at two levels with thresholds of 40 mV and 100 mV. This will allow the determination of effects from mis-counting beam positrons as muons.

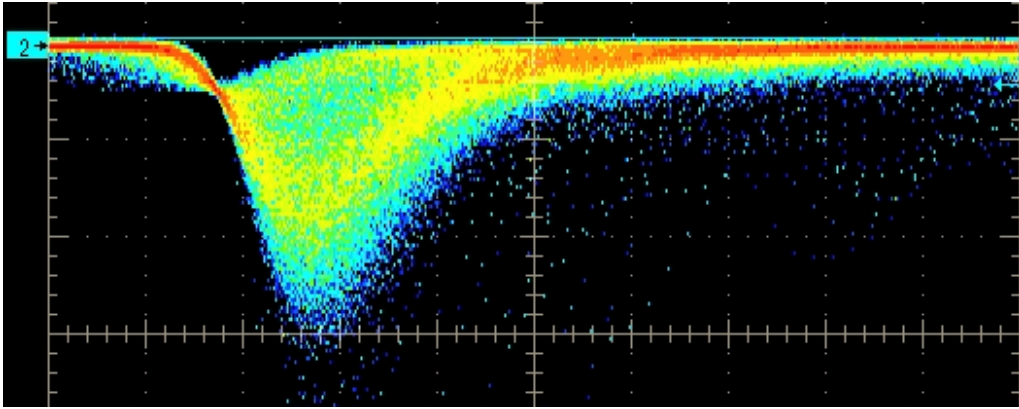


Figure 14. Trace of 500 μ m T0 scintillator. Bright yellow band is from beam muons. In contrast, the weak band just above oscilloscope trigger threshold is from beam positrons.

For two of our stopping targets, a permanent magnet assembly was used to produce a nearly homogeneous magnetic field of central value ≈ 85 G in the target region. The magnetic field was used to induce a μ SR signal at a known frequency. A non-depolarizing thin silver target was used to determine the amplitude of the μ SR signal from a polarized muon source. A 5 mm thick sulfur target—measured by us previously to depolarize muons by a factor of 12—was used

to reduce our sensitivity to μ SR. The third target was a thin sheet of AK-3, having an average internal magnetization of 1 T. This field is strong enough to produce a μ SR period much shorter than our temporal resolution and thus remove any detectable μ SR signal. The majority of the run was done with the AK-3 target. Fourier analysis of results obtained—first during a brief summer 2003 test, and later in the fall—revealed no discernable remanent frequency.

Since we were limited to the use of a *cw* beam we can either analyze the data in a "one-at-a-time" mode or use a multi-event method in producing lifetime histograms. The first method requires a cleaning window around each T0 hit; if a second T0 event is detected, neither can be used. This method produces a lower background contamination, but requires either a low beam rate so that most T0 events can be used or a loss of statistics at higher rates. The second method does not require a cleaning window, resulting in a larger background but can be used at any beam rate. In either case it is necessary to count all detector hits relative to each T0 event within a histogram window.

The analysis procedure has several steps. First we identify potential positron events in the detector by requiring a coincidence between an inner and an outer detector element. Then the times of each detector pair is compared to the T0 events to create a standard lifetime histogram. Using the silver data, with a strong μ SR signal, the phase and amplitude of oscillation is determined for each tile. This allows for adjustments to be made so that the point-like symmetric detector pairs can be added together with a minimal μ SR signal. Then, all of the histograms are summed to together to produce a final lifetime histogram. Finally, this histogram is fit with a multi-parameter function to determine the lifetime.

The focus of the analysis thus far has been with the multi-event method. Figure 15 shows a lifetime histogram generated using this method. The negative times are used only as diagnostics in analyzing the background. The large spike at the center of the histogram is due to prompt events in the T0 and detector. These type of events occur when a decay positron triggers the T0 scintillator and then hits a detector element. The positive half of the histogram is dominated by the exponential decay time and a flat background.

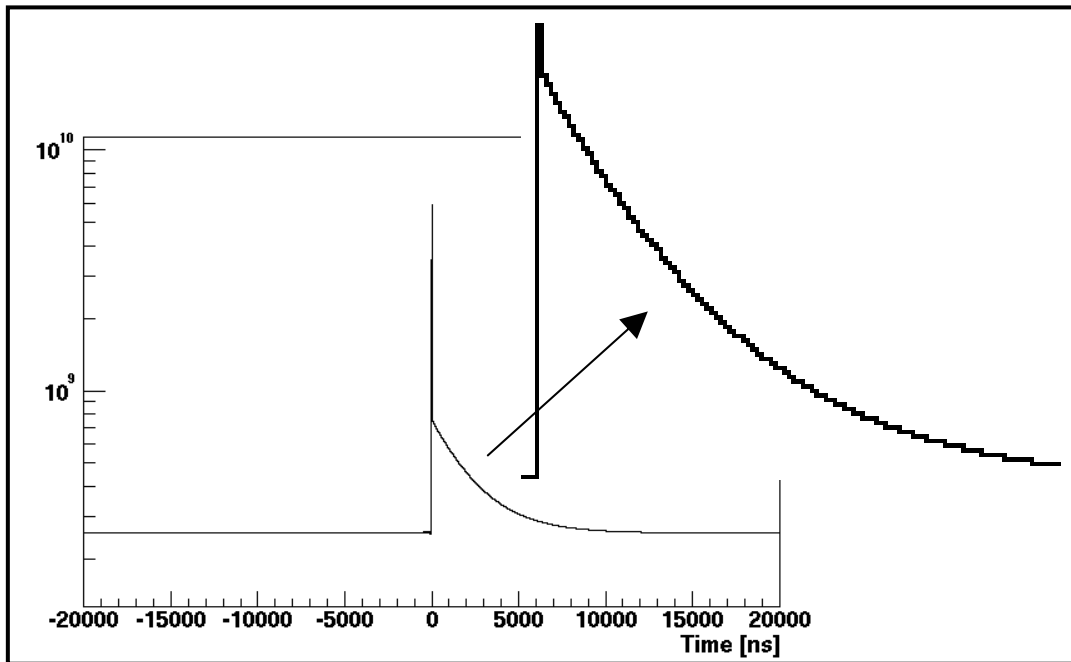


Figure 15. Lifetime data summed from all the runs in fall 2003.

In order to insure the measured lifetime is not being distorted by systematic effects we will perform several consistency checks. One test will be a start-time scan where we will vary the fit start time to determine that the variations in the measured lifetime is as expected from statistical fluctuations. A similar stop-time scan will also be implemented. Another test will be to perform the fit for various combinations of detectors such as by individual detector tiles, point-like symmetric pairs, houses, and hemispheres. In addition, we have different targets and rates to insure consistent results over those parameters. Finally, data sets were obtained over several weeks allowing for the determination of any long term systematic effects.

Estimate of precision on lifetime for each target and rate in ppm.

	Silver	Sulfur	AK3	Totals
Very Low Rate 30 - 40 kHz	-	-	97	97
Low Rate 45 - 60 kHz	175	-	52	50
Mid Rate 100 - 130 kHz	112	66	55	40
High Rate 300 - 450 kHz	211	81	74	53
Ultra High Rate > 500 kHz	-	130	165	102
Totals	86	48	31	25

Figure 16. Summary of data collected and estimated uncertainty on the muon lifetime.

Beamtime Request for 2004

The μ Lan Collaboration is requesting one six-week long run in the π E3 line, ideally scheduled during the last months of scheduled beam time. The length and scheduling are motivated by the following considerations:

Run Duration—Six Weeks

We anticipate commissioning two important and technologically challenging subsystems to our experiment: the pulsed kicker and the bank of waveform digitizers. Additionally, supporting systems, such as an expanded DAQ and data storage farm will be necessary. We will utilize new beam-monitoring wire chambers, and a new target system. Based on our past experience in π E3, we estimate 1 week for ordinary beam tuning, optimizing the final tune for best extinction fraction—these tests were cut short in our July run because of a kicker power supply failure. These tests will use the kicker in *dc* mode. We will use 1 – 2 weeks to focus on beam quality measurements and characterization with the pulsed kicker; during this time, we expect to have to make some adjustments to the electronic shielding of the detectors or cables, depending on the noise feedthrough in this real operation mode. We will also be debugging our detector electronics and readout during this new fast-switching operation. Calibration of the detectors and

background and alternative target runs will require 1 week. Finally, we reserve up to 2 – 3 weeks for “production” running using a variety of incident rates and target selections.

Run Scheduling—Late Fall

The kicker is being shipped to TRIUMF with expected arrival not before March 15. We have been advised to expect up to four months for assessment, modification and tests. Allowing a contingency of 50% (two months), and several weeks to pack, ship and install at PSI, the earliest time we could plan to run would be September 15. Later in the fall increases the contingency factor, obviously a plus from our side.

Our experiment is designed to use exclusively a large set of custom waveform digitizers. Problems to date with a simple part of the prototype board—the VME interface logic—have delayed our test and production schedule. Anticipating success in the next few months, we still require approximately five months for production and testing of the 85 units required for the run. Once several working prototypes are built, we can begin our final DAQ development using the new WFD boards. Completion of these tasks can be expected to take at least two months following full WFD production completion. Thus, early fall is the *earliest* we would feel comfortable scheduling any run that uses the new WFDs.

The other items on our “to do” list are more conventional and do not drive the schedule. However, the two central items discussed above combine to urge us to request as late a scheduling as possible this year. Last year, against our request, the *μLan* commissioning run was held in early fall, just before the target change and shortly after our summer beam test. The problems with the kicker—found during the summer run—had no real chance to be solved before the fall run. We were forced to set aside work on the kicker RF to focus on completion of the detector and use of the fall data taking in *cw* beam mode. We urge the committee to give high priority to our request to run near the end of 2004, thereby maximizing our chances to have both missing components to our project ready. With success, we would then be in a position to request an full production run at the beginning of summer 2005 with a fully working experiment.

Finally, *μLan* can make a very productive effort this year if either the kicker *or* the WFDs are ready. If only the kicker is ready, we will continue to use conventional discriminators and the CAEN TDCs for readout. This is a straight-forward task; at a precision of 3 ppm, we do not anticipate a problem with the approach. If, on the other hand, only the WFDs are ready, we will still learn a tremendous amount about the quality of the data with the full readout information provided by the digitizers. Of course, we are planning for success: we expect both items to be ready in fall 2004.

ⁱ R. M. Carey, M. Hare, W. Earle, E., Hazen, J. Miller, O. Rind, B.L. Roberts, *Boston University*, P. Debevec, F. E. Gray, D.W. Hertzog, C.J.G. Onderwater, C.C. Polly, M. Sossong, D.C. Urner, S. Williamson, *University of Illinois at Urbana-Champaign*, P. Cushman, *University of Minnesota*; “A Precision Measurement of the Positive Muon Lifetime Using a Pulsed Muon Beam and the *μLan* Detector,” Expt. R-99-07.1. Available on the Web at <http://www.npl.uiuc.edu/exp/mulan/muLanMain.html>